energies

MDPI

Article

Induction Machine Control for a Wide Range of Drive Requirements

Bojan Grčar [1,*], Anton Hofer [2] and Gorazd Štumberger [1]

[1] Faculty of Electrical Engineering and Computer Science, University of Maribor, Koroška 46, 2000 Maribor, Slovenia; gorazd.stumberger@um.si

[2] Institute of Automation and Control, Graz University of Technology, Inffeldgasse 21/B, 8010 Graz, Austria; anton.hofer@tugraz.at

* Correspondence: bojan.grcar@um.si

Received: 24 October 2019; Accepted: 23 December 2019; Published: 31 December 2019

check for updates

Abstract: In this paper, a method for induction machine (IM) torque/speed tracking control derived from the 3-D non-holonomic integrator including drift terms is proposed. The proposition builds on a previous result derived in the form of a single loop non-linear state controller providing implicit rotor flux linkage vector tracking. This concept was appropriate only for piecewise constant references and assured minimal norm of the stator current vector during steady-states. The extended proposition introduces a second control loop for the rotor flux linkage vector magnitude that can be either constant, programmed, or optimized to achieve either maximum torque per amp ratio or high dynamic response. It should be emphasized that the same structure of the controller can be used either for torque control or for speed control. Additionally, it turns out that the proposed controller can be easily adapted to meet different objectives posed on the drive system. The introduced control concept assures stability of the closed loop system and significantly improves tracking performance for bounded but arbitrary torque/speed references. Moreover, the singularity problem near zero rotor flux linkage vector length is easily avoided. The presented analyses include nonlinear effects due to magnetic saturation. The overall IM control scheme includes cascaded high-gain current controllers based on measured electrical and mechanical quantities together with a rotor flux linkage vector estimator. Simulation and experimental results illustrate the main characteristics of the proposed control.

Keywords: induction machines; nonlinear control; energy efficiency; torque/speed control

---

1. Introduction

Squirrel cage induction machines (IM) are widely used in various industrial applications, machining, transportation, and electrical vehicles. They are relatively simply constructed and therefore easy to produce but quite difficult to control, especially if high performance and energy efficiency are required. Field oriented control (FOC) and direct torque control (DTC) schemes with many modifications introduced to fulfill different control objectives are widely accepted by the industry. Following the progress in non-linear control theory, several propositions based on feedback linearization, passivity, and flatness [1–4] were introduced in the past. These concepts facilitate deeper understanding of nonlinear IM dynamics and improve feedback performance and robustness but are often quite difficult to design and to implement. As a consequence, a great number of modifications and extensions have been proposed for basic FOC and DTC to improve overall performance, efficiency, and robustness along with new estimation techniques [5–10].

It is a long term goal to develop IM control strategies which are able to meet increasing efficiency requirements, i.e., controllers which can produce prescribed torque trajectories while minimizing the power losses. For example, in [11] an optimal torque controller for an IM with a linear magnetic characteristic was proposed based on the calculus of variations. A quite different approach was presented in [12]. Introducing a general *steady state* model suitable for induction motors, permanent-magnet synchronous motors, reluctance synchronous motors, and DC motors, the problem of power loss minimization including core saturation is considered. In [13] a control strategy is proposed based on ideas similar to [11]. The problem of missing information about the future reference torque trajectory is removed assuming simple first order transients between constant reference torque phases. The online implementation requires the solution of a small static optimization problem. The problem of power loss minimization for step changes of the torque reference trajectory is also considered in [14]. In addition to [13] saturation effects of the main inductance are taken into account and a simplified suboptimal solution avoiding an online optimization is presented. Recently a quite different control scheme for a permanent magnet synchronous machine was given in [15]. Based on an linearized parameter dependent mathematical model for the motor which also includes magnetic saturation, a model predictive control concept is developed. The online optimization problem is solved by the projected fast gradient method.

In this paper, a new control concept based on 3-D non-holonomic (NH) integrator including drift terms is proposed. Using standard modeling assumptions and assuming "perfect" current control, a reduced IM (current) model can be written in the general NH integrator form. From the control standpoint NH systems, which originate in mechanics, are quite challenging since they fail to fulfill the necessary conditions for stabilization with a smooth state feedback [16]. For this class of systems, control schemes based on discontinuous feedback (hybrid, sliding mode, and time optimal), time-varying state feedback (trajectory planning, back-stepping, pattern generation) were proposed in [17–20]. In [21] the authors introduced a non-linear state controller based on NH system analysis applied to IM torque control. Considering the non-holonomic constraint requiring periodic orbits of the rotor flux linkage and stator current vectors, the proposed feedback assured global asymptotic stability and maximal torque/amp ratio in steady states for the nominal parameter case. An essential characteristic of the proposed control scheme is implicit rotor flux linkage tracking provided by the adjusted amplitude and frequency modulation of the stator current vector. Two main limitations were observed for the proposed control: only piecewise *constant* references were allowed and the problem of singularity (zero rotor flux) required an additional time optimal flux controller and a switching logic to provide soft transitions between the two regimes [22].

This contribution is based on the results given in [23] for the control of the general 3-D-nonholonomic integrator with drift. The main focus of the present paper is the adaption of the control concept presented in [23] for the usage in IM torque and speed control applications. For this purpose a nonlinear flux model is included and the problem of flux optimization in order to achieve the maximum torque per ampere feature is considered from the practical point of view. It is shown that a simple suboptimal strategy for the adjustent of the flux magnitude can be applied to a wide range of torque reference scenarios as well as to speed control tasks. The control input is consequently composed of two orthogonal components, the first providing the required rotor flux linkage vector and the second producing the desired torque. In this way the overall control structure becomes partially similar to FOC but without relying on the uncertain rotor flux reference frame. The proposed structure enables the rotor flux linkage vector to be either constant, programmed, or optimized for energy efficiency with respect to drive characteristics and requirements. Due to similarities with widespread FOC, the proposed control scheme can be easily implemented on a standard industrial hardware.

The presentation of the results is structured as follows. In Section 2, the basic IM model is introduced in the rotor reference frame. The resulting reduced current model along with a dynamic torque estimation constitute a general 3-D non-holonomic integrator that is used to introduce the basic nonlinear state controller. Section 3 shows how the basic control structure can be extended in order to provide improved tracking performance. A proof of the stability of the resulting closed loop system is given. In Section 4 the mathematical description of the IM is extended by a simple nonlinear flux model covering the phenomenon of magnetic saturation. Next, the problem of rotor flux magnitude optimization is addressed, such that torque tracking of the IM is performed efficiently. Different classes of torque reference signals are considered and appropriate solutions are given. Section 5 is dedicated to extensions of the controller structure and the task of speed control. In Section 6, implementation aspects and experimental results confirming the improved tracking performance for torque and speed control are discussed. Concluding remarks are given in Section 7.

2. Im Model and Basic Controller

Using a standard modeling approach the two-axis dynamic model of a 2-pole IM model written in an arbitrary d-q reference frame is given by

$$\begin{aligned}\dot{\mathbf{i}}_{d,q} &= \left(-\tau_\sigma^{-1}\mathbf{I} - \mathbf{J}\omega_s\right)\mathbf{i}_{d,q} + \left(\frac{M}{L_r L_\sigma \tau_r}\mathbf{I} - \frac{\omega_m M}{L_r L_\sigma}\mathbf{J}\right)\boldsymbol{\psi}_{d,q} \\ &\quad + L_\sigma^{-1}\mathbf{u}_{d,q} \\ \dot{\boldsymbol{\psi}}_{d,q} &= \left(-\tau_r^{-1}\mathbf{I} - \mathbf{J}(\omega_s - \omega_m)\right)\boldsymbol{\psi}_{d,q} + \frac{M}{\tau_r}\mathbf{i}_{d,q} \\ T_{el} &= \frac{M}{L_r}\left(\psi_d i_q - \psi_q i_d\right),\end{aligned} \tag{1}$$

where $\mathbf{i}_{d,q}$, $\mathbf{u}_{d,q}$, $\boldsymbol{\psi}_{d,q}$ are the stator current vector, the stator voltage vector, and the rotor flux linkage vector written in the d-q reference frame. The mutual inductance is denoted by M, L_r is the rotor inductance, R_r is the rotor resistance, ω_m is the rotor speed, ω_s is the speed of the d-q reference frame with respect to the stator, T_{el} is the electric torque while $\mathbf{I}$ is the 2×2 identity matrix and $\mathbf{J}$ is the 2×2 skew symmetric rotational matrix. The leakage inductance L_σ, the resistance R_σ, the rotor time constant τ_r and the leakage time constant τ_σ are defined as $L_\sigma = L_s - M^2/L_r,\ R_\sigma = R_s - (R_r M)^2/L_r^2$, $\tau_r = L_r/R_r$ and $\tau_\sigma = L_\sigma/R_\sigma$. Throughout the text references, estimated variables and errors values are denoted as $(.)^*$, $\widehat{(.)}$, $\widetilde{(.)}$.

Under the assumption of a perfect current control, i.e., $\mathbf{i}_{d,q} = \mathbf{i}^*_{d,q}$, the simplified IM (current) model written in the rotor reference frame γ-δ is obtained from the model written in (1) by considering $\omega_m = \omega_s$ and changing d to γ and q to δ:

$$\dot{\boldsymbol{\psi}}_{\gamma,\delta} = -\tau_r^{-1}\boldsymbol{\psi}_{\gamma,\delta} + \frac{M}{\tau_r}\mathbf{i}_{\gamma,\delta} \tag{2}$$

where $\mathbf{i}_{\gamma,\delta}$ are control inputs, while the machine torque represents the controlled variable. For torque control the output error is defined as $\tilde{T}_{el} := T^*_{el} - \hat{T}_{el}$, where the actual machine torque T_{el} in (1) is replaced by a filtered estimate

$$\tau_f \dot{\hat{T}}_{el} = -\hat{T}_{el} + \frac{M}{L_r}\left(\psi_\gamma i_\delta - \psi_\delta i_\gamma\right). \tag{3}$$

In this model $\tau_f \ll \tau_r$ is the filter time constant, that is introduced to capture the estimation dynamics and to remove higher frequency components generated by estimation process and measurement of stator currents. A standard singular perturbation argument involving the estimation time constant τ_f recovers the algebraic expression for the actual machine torque. Equations (2) and (3) constitute the general 3-D non-holonomic integrator that includes drift terms.

Using the output error $\tilde{T}_{el}$ and the abbreviation $s_3 := \mathrm{sign}(T^*_{el})$ with the convention $T^*_{el} = 0 \rightarrow s_3 = 0$, the basic nonlinear state controller was proposed in [21] as:

$$\begin{bmatrix} i_\gamma \\ i_\delta \end{bmatrix} = \frac{\tau_r}{M}\begin{bmatrix} \frac{1}{\tau_r} + s_3 k_p \tilde{T}_{el} & -\left(\frac{s_3}{\tau_r} + k_p \tilde{T}_{el}\right) \\ \frac{s_3}{\tau_r} + k_p \tilde{T}_{el} & \frac{1}{\tau_r} + s_3 k_p \tilde{T}_{el} \end{bmatrix}\begin{bmatrix} \psi_\gamma \\ \psi_\delta \end{bmatrix} \tag{4}$$

where $k_p > 0$ denotes a controller gain. The terms that are output error independent compensate the drift terms and provide purely oscillatory dynamics of the rotor flux linkage vector $\boldsymbol{\psi}_{\gamma,\delta}$ as the output error $\tilde{T}_{el}$ vanishes. On the other hand, the terms that are output error dependent provide the adjusted amplitude and frequency modulation of the input current vector. The feedback system is obtained from (2) to (4) in the following form:

$$\begin{aligned} \dot{\psi}_\gamma &= s_3 k_p \tilde{T}_{el} \psi_\gamma - \left(s_3 \tau_r^{-1} + k_p \tilde{T}_{el} \right) \psi_\delta \\ \dot{\psi}_\delta &= \left(s_3 \tau_r^{-1} + k_p \tilde{T}_{el} \right) \psi_\gamma + s_3 k_p \tilde{T}_{el} \psi_\delta \\ \dot{\hat{T}}_{el} &= -\tau_f^{-1} \hat{T}_{el} + \tau_f^{-1} \frac{\tau_r}{L_r} \left(s_3 \tau_r^{-1} + k_p \tilde{T}_{el} \right) \left(\psi_\gamma^2 + \psi_\delta^2 \right) \end{aligned} \tag{5}$$

In [21] it was proven that (5) has the following properties: For any constant $T_{el}^* \neq 0$, any $\hat{T}_{el}(0)$ and $\boldsymbol{\psi}_{\gamma,\delta}(0) \neq \mathbf{0}$ the system converges to a state where $\hat{T}_{el} = T_{el}^*$ and the components of $\boldsymbol{\psi}_{\gamma,\delta}(t)$ are harmonic functions with the amplitude

$$\left\| \boldsymbol{\psi}_{\gamma,\delta} \right\|_2 = \sqrt{L_r \left| T_{el}^* \right|}.$$

and the angular frequency $s_3 \tau_r^{-1}$. Furthermore, a distinctive characteristic of (5) is that, for a given piecewise constant output reference T_{el}^* the minimal norm of the control input vector $\mathbf{i}_{\gamma,\delta} = \left[\begin{array}{cc} i_\gamma & i_\delta \end{array} \right]^T$ is assured in steady states

$$\left\| \mathbf{i}_{\gamma,\delta} \right\|_2 = \sqrt{2 \frac{L_r}{M^2} \left| T_{el}^* \right|}.$$

The angle between the rotor flux vector and the stator current is $s_3 \pi / 4$ *permanently* as was already presented in [21]. The rotation speed of the stator current vector is obtained as $\omega_I = \omega_r + \omega_m$, where the introduced "relative" speed ω_r corresponds to the inverse time rotor constant τ_r^{-1}. The relative speed exactly matches the slip speed in steady states. Further remarks and characteristics of the controlled system (5) regarding stability, robustness, singularity avoidance, and overall performance can be found in [21,22].

3. Improved Torque Tracking Controller

Since from now on all vectors are expressed as vectors in the rotor reference frame the index combination γ, δ is omitted. The main characteristic of the presented basic controller, namely the implicit rotor flux tracking without separate control loop works perfectly for a piecewise constant torque references assuring also maximal torque-per-amp ratio. The main obstacle for a good tracking performance in general is observed especially at zero crossings of T_{el}^* with finite slope since the magnitude of the rotor flux linkage becomes too small or even zero. This results in the output $\hat{T}_{el}$ getting out of control for a short period as can easily be seen from the third equation in (5).

3.1. Controller Modification

To cope with this problem the basic controller scheme (4) has to be conceptually modified. Based on the ideas outlined in [23] the control input is composed of two orthogonal parts

$$\mathbf{i} = \mathbf{i}_\psi + \mathbf{i}_\tau \tag{6}$$

where the vector $\mathbf{i}_\psi$ influences only the rotor flux linkage magnitude ψ, whereas the vector $\mathbf{i}_\tau$ facilitates machine torque. Considering the basic control structure it is intended that the effect of the diagonal elements in (4) is replaced by an appropriately selected vector $\mathbf{i}_\psi$. The presentation of the control design can be simplified if polar coordinates are introduced for the rotor flux vector

$$\psi_\gamma = \psi \cos \varphi \qquad \psi_\delta = \psi \sin \varphi \tag{7}$$

with

$$\psi = \|\boldsymbol{\psi}_{\gamma,\delta}\|_2 = \sqrt{\psi_\gamma^2 + \psi_\delta^2} \quad \varphi = \arctan\left(\frac{\psi_\delta}{\psi_\gamma}\right). \tag{8}$$

The plant Equations (2) and (3) are then obtained as:

$$\dot{\psi} = -\tau_r^{-1}\psi + \tau_r^{-1}M\left(i_\gamma \cos\varphi + i_\delta \sin\varphi\right) \tag{9}$$

$$\psi\dot{\varphi} = \tau_r^{-1}M\left(-i_\gamma \sin\varphi + i_\delta \cos\varphi\right) \tag{10}$$

$$\dot{\hat{T}}_{el} = -\tau_f^{-1}\hat{T}_{el} + \tau_f^{-1}\frac{M}{L_r}\left(-i_\gamma \sin\varphi + i_\delta \cos\varphi\right)\psi \tag{11}$$

$$T_{el} = \frac{M}{L_r}\left(-i_\gamma \sin\varphi + i_\delta \cos\varphi\right)\psi \tag{12}$$

Now it is obvious that the control vector $\mathbf{i}_\psi$ must be of the form

$$\mathbf{i}_\psi = \begin{bmatrix} i_{\psi\gamma} \\ i_{\psi\delta} \end{bmatrix} = \begin{bmatrix} I\cos\varphi \\ I\sin\varphi \end{bmatrix}$$

with a suitable selected magnitude I in order to influence the flux magnitude ψ only. Introducing the reference signal ψ^* for the rotor flux linkage magnitude ψ a simple proportional control is proposed for the "magnetizing" vector $\mathbf{i}_\psi$

$$\mathbf{i}_\psi = \frac{1}{M}\begin{bmatrix} \left(\psi^* + k_\psi(\psi^* - \psi)\right)\cos\varphi \\ \left(\psi^* + k_\psi(\psi^* - \psi)\right)\sin\varphi \end{bmatrix}, \tag{13}$$

where $k_\psi > 0$ is a tuning parameter and $\psi^* > 0$ is assumed. By inserting (13) in (9) it follows that the rotor flux magnitude is ψ driven by the linear first order dynamics with unit gain:

$$\dot{\psi} = -\tau_r^{-1}(1+k_\psi)\psi + \tau_r^{-1}(1+k_\psi)\psi^* \tag{14}$$

The time constant of (14) can be simply influenced by an appropriate selection of the parameter k_ψ. It is important to note that (14) is completely decoupled from the other two states φ, $\hat{T}_{el}$.

Since $\mathbf{i}_\psi$ should replace the effect of the diagonal elements in (4) the second control vector $\mathbf{i}_\tau$ influencing only the output error results from the remaining part of (4):

$$\begin{aligned} \mathbf{i}_\tau &= \frac{\tau_r}{M}\begin{bmatrix} -\left(s_3\tau_r^{-1} + k_p\tilde{T}_{el}\right)\psi_\delta \\ \left(s_3\tau_r^{-1} + k_p\tilde{T}_{el}\right)\psi_\gamma \end{bmatrix} \\ &= \frac{\tau_r}{M}\begin{bmatrix} -\left(s_3\tau_r^{-1} + k_p\tilde{T}_{el}\right)\psi\sin\varphi \\ \left(s_3\tau_r^{-1} + k_p\tilde{T}_{el}\right)\psi\cos\varphi \end{bmatrix} \end{aligned} \tag{15}$$

Obviously $\mathbf{i}_\tau$ has no effect on the flux magnitude ψ. By inserting (15) into (10), it follows

$$\dot{\varphi} = s_3\tau_r^{-1} + k_p\tilde{T}_{el}.$$

When the torque error $\tilde{T}_{el}$ vanishes the rotor flux linkage dynamics results in a harmonic oscillator with an angular speed $\dot{\varphi} = s_3\tau_r^{-1}$. This property which is implicitly contained in the basic controller (4) is reasonable only for piecewise *constant* references T_{el}^* but it is too restrictive in general. Therefore, it is proposed to replace the term $s_3\tau_r^{-1}$ in (15) with the expression

$$R_r\frac{T_{el}^*}{(\psi^*)^2} \quad \text{(with the restriction } \psi^* > 0\text{)}.$$

One of the reasons for this replacement is the fact that in the case of a constant reference T^*_{el} and the choice $\psi^* = \sqrt{L_r \left|T^*_{el}\right|}$ the same steady state is obtained as by using the basic controller (4). This means that the important property of (4), i.e., producing a constant torque with minimum norm of the control input is recovered by the modified controller. Finally, by combining (13) and (15) (with the proposed modification), a new control law is obtained:

$$\begin{aligned} i_\gamma &= \frac{\tau_r}{M}\Big[-(R_r\tfrac{T^*_{el}}{(\psi^*)^2} + k_p\tilde{T}_{el})\psi\sin\varphi. \\ &\quad + \tau_r^{-1}\left(\psi^* + k_\psi(\psi^*-\psi)\right)\cos\varphi\Big] \\ i_\delta &= \frac{\tau_r}{M}\Big[(R_r\tfrac{T^*_{el}}{(\psi^*)^2} + k_p\tilde{T}_{el})\psi\cos\varphi. \\ &\quad + \tau_r^{-1}\left(\psi^* + k_\psi(\psi^*-\psi)\right)\sin\varphi\Big] \end{aligned} \tag{16}$$

The resulting closed loop system built up by (9)–(11), (16) is given as:

$$\begin{aligned} \dot{\psi} &= -\tau_r^{-1}(1+k_\psi)\psi + \tau_r^{-1}(1+k_\psi)\psi^* \\ \dot{\varphi} &= R_r\frac{T^*_{el}}{(\psi^*)^2} + k_p\tilde{T}_{el} \\ \dot{\hat{T}}_{el} &= -\tau_f^{-1}(1+\frac{k_p}{R_r}\psi^2)\hat{T}_{el} + \tau_f^{-1}(\frac{\psi^2}{(\psi^*)^2} + \frac{k_p}{R_r}\psi^2)T^*_{el} \end{aligned} \tag{17}$$

Of course the control law (16) can be transformed back into the original state variable form by the inverse relations (7) and (8). Which, in combination with the plant model (2) and (3) leads to the following description of the closed loop system:

$$\begin{aligned} \dot{\psi}_\gamma &= -\tau_r^{-1}\psi_\gamma - \left(R_r\frac{T^*_{el}}{(\psi^*)^2} + k_p\tilde{T}_{el}\right)\psi_\delta \\ &\quad + \tau_r^{-1}\left(\psi^* + k_\psi\left(\psi^* - \sqrt{\psi_\gamma^2+\psi_\delta^2}\right)\right)\frac{\psi_\gamma}{\sqrt{\psi_\gamma^2+\psi_\delta^2}} \\ \dot{\psi}_\delta &= -\tau_r^{-1}\psi_\delta - \left(R_r\frac{T^*_{el}}{(\psi^*)^2} + k_p\tilde{T}_{el}\right)\psi_\gamma \\ &\quad + \tau_r^{-1}\left(\psi^* + k_\psi\left(\psi^* - \sqrt{\psi_\gamma^2+\psi_\delta^2}\right)\right)\frac{\psi_\delta}{\sqrt{\psi_\gamma^2+\psi_\delta^2}} \\ \dot{\hat{T}}_{el} &= -\tau_f^{-1}\hat{T}_{el} + \frac{\tau_f^{-1}}{R_r}\left(R_r\frac{T^*_{el}}{(\psi^*)^2} + k_p\tilde{T}_{el}\right)\left(\psi_\gamma^2+\psi_\delta^2\right) \end{aligned} \tag{18}$$

3.2. Stability Analysis

Since the closed loop system has two external inputs it must be proven that the norm of the state vector $\mathbf{x} = \begin{bmatrix} \psi_\gamma & \psi_\delta & \hat{T}_{el} \end{bmatrix}^T$ remains bounded whenever the norm of the input vector defined as $\mathbf{r} := \begin{bmatrix} \psi^* & T^*_{el} \end{bmatrix}^T$ and $\|\mathbf{x}(\mathbf{0})\|_2$ are bounded. This task becomes much easier, if the model (17) is used. Obviously we have

$$\|\mathbf{x}\|_2^2 = \psi^2 + \hat{T}_{el}^2, \tag{19}$$

therefore only the first and the third equation of (17) have to be considered. Next, it is assumed that the following bounds hold for the external inputs

$$0 < \psi^*_{\min} \leq \psi^*(t) \leq \psi^*_{\max} \ \text{ for all } t \geq 0 \tag{20}$$

$$|T^*_{el}(t)| \leq T^*_{el,\max} \ \text{ for all } t \geq 0, \tag{21}$$

where $T^*_{el,\max}, \psi^*_{\min}, \psi^*_{\max}$ are some finite positive constants. With the restriction $k_\psi > 0$ it follows immediately from the first equation in (17) that

$$\psi(t) \leq e^{-\tau_r^{-1}(1+k_\psi)t}\psi(0) + \psi^*_{\max} \leq \psi(0) + \psi^*_{\max}. \tag{22}$$

Thus $\psi(t)$ remains bounded for any finite initial value $\psi(0) \geq 0$ and any external input $\psi^*(t)$ satisfying (20).

Now the third equation in (17) can be regarded as a linear *timevariant* first order system with the external input T^*_{el} and with the output $\hat{T}_{el}$. For the stability analysis of this system the homogeneous case (i.e., $T^*_{el} = 0$) is considered first which leads to:

$$\begin{aligned}\hat{T}_{el}(t) &= e^{\int_{t_0}^{t} -\tau_f^{-1}(1+\frac{k_p}{R_r}\psi^2)d\tau}\hat{T}_{el}(t_0) \\ &= e^{-\tau_f^{-1}(t-t_0)}e^{\int_{t_0}^{t} -\tau_f^{-1}\frac{k_p}{R_r}\psi^2 d\tau}\hat{T}_{el}(t_0)\end{aligned}$$

Taking into account $k_p > 0$, it follows

$$\left|\hat{T}_{el}(t)\right| \leq e^{-\tau_f^{-1}(t-t_0)}\left|\hat{T}_{el}(t_0)\right|,$$

which shows that the homogeneous system is uniformly exponentially stable. Furthermore from (20) to (22) we can derive the result

$$\tau_f^{-1}\left|\frac{\psi^2}{(\psi^*)^2} + \frac{k_p}{R_r}\psi^2\right| \leq c \ \text{ for all } t \geq 0$$

where c denotes some finite positive constant. This inequality combined with the fact that the homogeneous part is uniformly asymptotically stable assures that $|\hat{T}_{el}(t)|$ remains bounded, whenever $\left|T^*_{el}(t)\right|$ and $\hat{T}_{el}(0)$ are bounded [24]. Finally from (19) the desired result follows that $\|\mathbf{x}\|_2$ remains bounded. Furthermore, it is important to note that also the angular rotation speed $\dot{\varphi}$ of the rotor flux vector remains bounded (see second equation in (17)).

4. Magnetic Saturation and Flux Reference Optimization

The new control law (16) provides the flux reference signal ψ^* as an additional external input. In this section the problem how to choose ψ^* in order to achieve energy efficient tracking of a desired torque T^*_{el} will be tackled. Since we would like to take full advantage of the dynamic capabilities of the induction machine, magnetic saturation must be considered. A correct mathematical description of this phenomenon would lead to a very complicated model, useless for control design. Therefore, a simple approach proposed in [25] for field oriented control is adopted which is also applied in [26]. It is based on the magnetization curve of the induction machine given in the form

$$\psi = f(i_\psi), \tag{23}$$

where the magnetizing current i_ψ is defined as

$$i_\psi := i_\gamma \cos\varphi + i_\delta \sin\varphi. \tag{24}$$

It should be mentioned that $|i_\psi| = \|\mathbf{i}_\psi\|_2$ is valid. Simple geometric considerations based on the phasors $\mathbf{i}_{\gamma,\delta}$ and $\boldsymbol{\psi}_{\gamma,\delta}$ reveal that this relation holds, where $\mathbf{i}_\psi$ is defined in (6) and (13) respectively. The magnetization curve can be obtained by measurements (e.g., [26]). Throughout the rest of the paper M and L_r are the nominal values of the mutual inductance and rotor inductance below saturation.

The following nonlinear flux model was introduced in [25]

$$\dot{\psi} = \tau_r^{-1} M \left(-f^{-1}(\psi) + i_\psi \right), \tag{25}$$

where $f^{-1}(\psi)$ is the inverse magnetizing function. For the next considerations it is useful also to introduce the torque producing current component

$$i_\tau := -i_\gamma \sin\varphi + i_\delta \cos\varphi. \tag{26}$$

(with the property $|i_\tau| = \|\mathbf{i}_\tau\|_2$, given by the same geometric considerations as mentioned above), which allows us to write (12) in the form:

$$T_{el} = \frac{M}{L_r} i_\tau \psi \tag{27}$$

Note that the real electrical torque T_{el} is considered in the present case. The Equations (25) and (26) are the basis for the flux optimization problem. In the following subsection a piecewise constant torque reference T_{el}^* is considered and the corresponding optimization problem is solved. It is assumed that the desired torque can be produced by the IM within the given current and voltage limitations. The resulting optimal flux magnitude ψ_{opt} can be used as flux reference signal ψ^* in the proposed control structure.

4.1. Constant Reference T_{El}^*

In the first case, the following question is considered: How should the *constant* flux ψ be selected, so that a desired *constant* torque $T_{el} = T_{el}^* \neq 0$ is achieved with minimum norm of the current vector in steady state? In other words, we want to get the *maximum torque per amp* feature. If magnetic saturation is neglected (i.e., for the linear flux model) the solution is simple

$$\psi_{opt} = \sqrt{L_r \left| T_{el}^* \right|}, \tag{28}$$

was already mentioned in Section 3. In the saturation case we get from (23)

$$i_\psi = f^{-1}(\psi),$$

which is the necessary value of i_ψ in order to achieve the constant ψ in steady state. From (27) it follows

$$i_\tau = \frac{L_r}{M} \frac{T_{el}^*}{\psi}$$

and using the fact $\|\mathbf{i}\|_2^2 = i_\psi^2 + i_\tau^2$ the problem can be formulated as:

$$\psi_{opt} = \underset{\psi}{\operatorname{argmin}} \left(\left(f^{-1}(\psi) \right)^2 + \left(\frac{L_r}{M} \frac{T_{el}^*}{\psi} \right)^2 \right) \tag{29}$$

By differentiating with respect to ψ the necessary condition is obtained

$$2 f^{-1}(\psi) \frac{d f^{-1}(\psi)}{d\psi} - \frac{2 L_r^2}{M^2} \frac{T_{el}^{*2}}{\psi^3} \stackrel{!}{=} 0.$$

Unfortunately, this equation cannot be solved for ψ but this causes no severe problems since it can be written as:

$$L_r\,|T_{el}^*| = M\sqrt{\psi^3 f^{-1}(\psi)\frac{df^{-1}(\psi)}{d\psi}} =: g(\psi) \tag{30}$$

The function $g(\psi)$ can be evaluated and stored in a lookup table so that the desired result can be obtained numerically in the form

$$\psi_{opt} = g^{-1}(L_r\,|T_{el}^*|). \tag{31}$$

A comparison between the optimal flux magnitude based on (28) and (31) is shown in Figure 1b. A similar result was presented in [14] where power losses for torque steps were considered and a function, which determines the optimal constant flux magnitude for constant torque levels, is given.

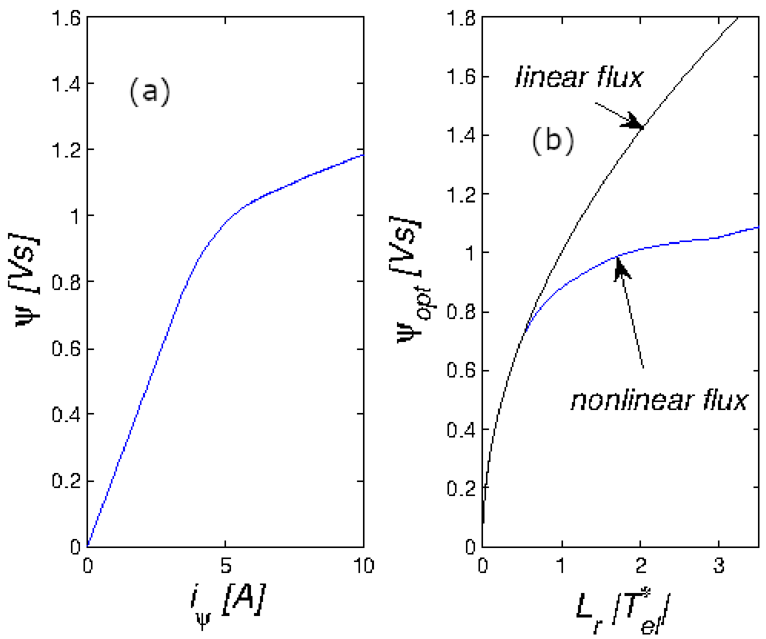

Figure 1. Magnetization curve (**a**); Optimal flux magnitude for constant torque (**b**).

4.2. General Case

In general, an arbitrary but bounded reference signal $T_{el}^*(t)$ defined over a finite time interval $0 \le t \le T_0$ is considered. In contrast to the forementioned case, a time function $\psi(t)$ should be determined now, so that the criterion

$$E = \int_0^{T_0} \left(i_\psi^2 + i_\tau^2\right) dt \tag{32}$$

is minimized for $T_{el}(t) = T_{el}^*(t)$. This means that the optimal flux trajectory $\psi(t)$ for an arbitrary torque reference signal should be determined. Obviously the value of E will also depend on the initial condition $\psi(0)$. In order to eliminate this influence, a periodic continuation of $T_{el}^*(t)$ is assumed and the steady state solution of the problem is considered. In this case $\psi(t)$ is a periodic time function too. From (27), it follows

$$i_\tau(t) = \frac{L_r}{M}\frac{T_{el}^*(t)}{\psi(t)} \tag{33}$$

and therefore the optimization problem can be formulated as:

$$\begin{aligned} &\text{mimimize} \int_{0}^{T_0} \left(i_\psi(t)^2 + \left(\frac{L_r}{M} \frac{T_{el}^*(t)}{\psi(t)} \right)^2 \right) dt \\ &\text{subject to} \\ &\dot{\psi} = \tau_r^{-1} M \left(-f^{-1}(\psi) + i_\psi \right) \\ &\psi(0) = \psi(T_0) \qquad i_\psi(0) = i_\psi(T_0). \end{aligned} \tag{34}$$

The boundary conditions are given by the fact that $\psi(t)$ and $i_\psi(t)$ must also be continuous functions. This flux optimization problem can be treated by the classical methods of optimal control (see e.g., [27]). First the Hamilton function is introduced (the argument time is omitted for brevity)

$$H = i_\psi^2 + \left(\frac{L_r}{M} \frac{T_{el}^*}{\psi} \right)^2 + \lambda \tau_r^{-1} M \left(-f^{-1}(\psi) + i_\psi \right), \tag{35}$$

where λ denotes a Lagrange multiplier. Now the solution of the problem must satisfy the following necessary conditions:

$$0 = \frac{\partial H}{\partial i_\psi} = 2 i_\psi + \lambda \tau_r^{-1} M \;\; \rightarrow \;\; i_\psi = -\frac{\lambda \tau_r^{-1} M}{2} \tag{36}$$

$$\dot{\lambda} = -\frac{\partial H}{\partial \psi} = 2 \left(\frac{L_r}{M} T_{el}^* \right)^2 \frac{1}{\psi^3} + \lambda \tau_r^{-1} M \frac{d f^{-1}(\psi)}{d\psi} \tag{37}$$

$$\dot{\psi} = \frac{\partial H}{\partial \lambda} = \tau_r^{-1} M \left(-f^{-1}(\psi) + i_\psi \right) \tag{38}$$

Substituting i_ψ in Equation (38) with the expression from Equation (36), the resulting boundary value problem is obtained:

$$\begin{aligned} \dot{\lambda} &= 2 \left(\frac{L_r}{M} T_{el}^* \right)^2 \frac{1}{\psi^3} + \lambda \tau_r^{-1} M \frac{d f^{-1}(\psi)}{d\psi} \\ \dot{\psi} &= \tau_r^{-1} M \left(-f^{-1}(\psi) - \frac{\lambda \tau_r^{-1} M}{2} \right) \\ \psi(0) &= \psi(T_0) \qquad \lambda(0) = \lambda(T_0) \end{aligned} \tag{39}$$

This problem can be solved numerically using appropriate software e.g., [28]. Finally, the optimal solution $\psi_{opt}(t)$ can be applied as flux reference signal $\psi^*(t)$. This solution could be implemented only if the reference trajectory is known in advance. A less restrictve assumption is discussed next.

In order to give more information about the solution of the boundary value problem (39), an example is presented. The parameters of the IM are taken from Table 1 and a reference torque $T_{el}^*(t)$ is chosen as shown in Figure 2a. The MATLAB function `bvp4c` was used to solve the boundary value problem. The resulting optimal flux magnitude $\psi_{opt}(t)$ is depicted in Figure 2b,c; it contains the corresponding current $i_\psi(t)$ and also the component $i_\tau(t)$ which is determined from the optimal solution by (33) with $\psi(t)$ replaced by $\psi_{opt}(t)$. The resulting value of the performance criterion (32) is given as $E = 336.04$.

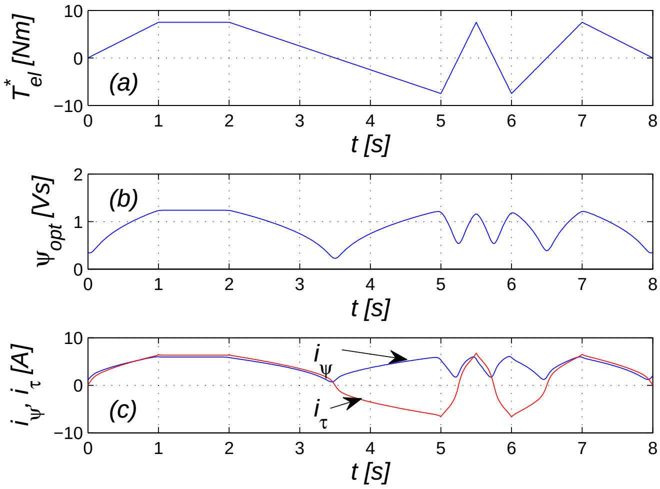

Figure 2. (**a**) Reference torque; (**b**) optimal flux magnitude; (**c**) optimal currents.

Table 1. Nominal motor data and controller parameters.

Symbol	Parameter	Value
P_n	nominal power	3 kW
U_n	supply voltage	220/380 V
I_n	nominal current	13/7.5 A
n_n	synchronous speed	1328 rpm
R_s	stator resistance	1.97 Ω
R_r	rotor resistance	2.91 Ω
L_s	stator inductance	0.2335 H
L_r	rotor inductance	0.2335 H
M	mutual inductance	0.223 H
L_σ	leakage inductance	0.0105 H
T_{el}	nominal torque	10 Nm
J	drive inertia	0.031 kgm^2
c	friction constant	0.025 Nms/rad
α	saturation parameter	0.13
β	saturation parameter	1.7154
τ_f	filter time-constant	0.005 s
k_ψ	flux controller gain	1.5
k_p	torque controller gain	2.5
k_p	speed controller gain	25
k_{pi}	current controller gain	20
k_{ii}	integrator gain	225.5

5. Final Controller Modifications

In the previous section two different scenarios concerning the torque reference signal T^*_{el} were investigated. The general case—being the most interesting one—needs the solution of a nonlinear boundary value problem. In this case the torque reference signal must be known in advance which drastically limits the applicability. Therefore, a suboptimal but easily implementable method for the selection of the flux reference signal ψ^* is preferred. A very simple but nevertheless reasonable possibility can be derived by a comparison of the optimization problems (29) and (34). In addition to the boundary conditions, the two problems differ mainly in the fact that the *dynamic* flux model is taken into account in (34). If replaced by the *static* flux model (23) a similar functional as in (29) is obtained. Based on the result (31) for problem (29) the following choice

$$\psi^*(t) = g^{-1}\left(L_r \left|T^*_{el}(t)\right|\right)$$

is introduced for the general case. In [14] the special case of step changes in the reference torque (or step changes filtered by a stable linear second order system) are considered. The optimization problem for the flux magnitude in order to minimize the power losses is formulated. Finally, the optimization problem is simplified in the way that only the constant power losses in steady state are taken into account. For proposed solution it should be emphasized that $\psi^*(t)$ is applied for general torque trajectories. Obviously this selection of the flux reference is optimal in the case of piecewise constant reference torques but it requires certain limitations in order to meet the requirements in the general case. Therefore, it is proposed to use

$$\psi^*(t) = \mathrm{sat}\left(g^{-1}\left(L_r \left|T^*_{el}(t)\right|\right), \psi^*_{\min}, \psi^*_{\max}\right), \tag{40}$$

where the saturation function is defined as

$$y = \mathrm{sat}\left(x, x_{\min}, x_{\max}\right) := \begin{cases} x_{\min} \ \text{ if } x < x_{\min} \\ x \ \text{ if } \ x_{\min} \le x \le x_{\max} \\ x_{\max} \text{ if } x > x_{\max} \end{cases}.$$

The lower bound $\psi^*_{\min} > 0$ has to be introduced in order to avoid the problems at zero crossings of $T^*_{el}(t)$ as mentioned in Section 3. Of course it is not possible to give an exact bound on the "suboptimality" of the proposed flux reference strategy for an arbitrary torque reference signal which is not given in advance. However, the choice of the lower bound $\psi^*_{\min}$ offers a simple way to adjust the concept to the expected reference torque trajectories. Especially in the case of slowly varying reference torques the efficiency improvement can be significantly compared to the constant flux reference case as can be seen in Figure 2. Upper bound $\psi^*_{\max}$ should prohibit unduly high magnetization or can be used in the field weakening range being defined as a function of the rotor speed ω_m. The introduction of the lower bound ψ^*_{min} for the flux reference signal is helpful to meet different drive requirements. In cases where the dynamics of the torque response is of main interest an operation with constant flux magnitude may be preferable which can be obtained by setting $\psi^*_{min} = \psi^*_{max}$. On the other hand, if efficiency of the drive is emphasized a small value of ψ^*_{min} will be a suitable choice. Of course, in cases where the required torque $T^*_{el}(t)$ is known in advance (e.g., in robotic applications) the optimal flux reference $\psi^*(t)$ resulting from the boundary value problem (39) can be applied directly, i.e., the first equation of the controller (41) can be omitted.

The results obtained by this simple approach are shown in Figure 3. The same torque reference signal $T^*_{el}(t)$ as used in the previous example leads to a flux reference signal $\psi^*(t)$ nearly coinciding with the optimal flux $\psi_{opt}(t)$ most of the time. Here the bounds were chosen somewhat arbitrarily as $\psi^*_{\min} = 0.35$ and $\psi^*_{\max} = 1.4$. Interestingly, the performance criterion only marginally deteriorates compared to the optimal solution. In this case the value is given as $E = 337.6$. Considering the torque reference signal in Figure 2a and the deviation from the optimal flux in Figure 3c it follows that high dynamic changes in the reference torque require an increasing value of the lower bound $\psi^*_{\min}$ in order to get a good approximation of the optimal flux magnitude.

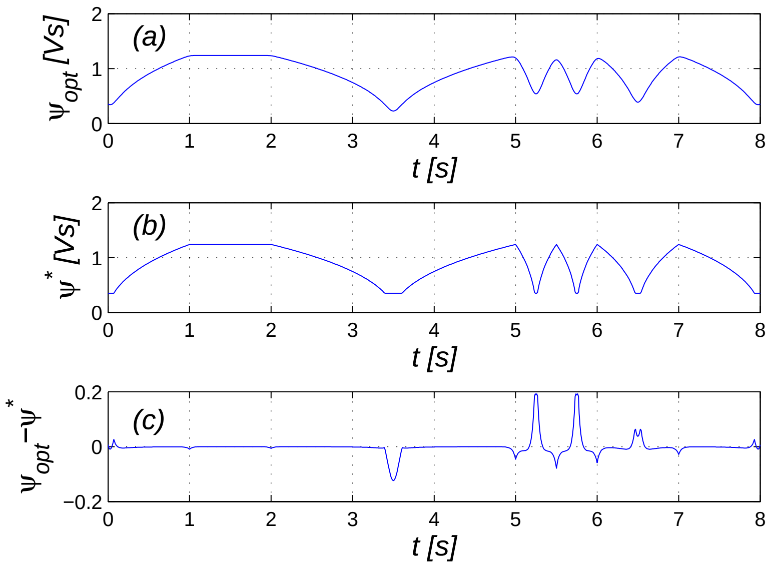

Figure 3. (**a**) Optimal flux magnitude; (**b**) flux reference resulting from (40); (**c**) deviation from optimal flux.

The inclusion of the nonlinear flux model (25) into the control concept requires a minor modification of (13). The feedforward part ψ^*/M in this scheme must be replaced by the inverse magnetization function in order to achieve the correct flux magnitude.

Thus, the torque controller is proposed in its final form as follows: given the reference torque $T^*_{el}(t)$ as external input, the estimated torque $\hat{T}_{el}(t)$ and the flux coordinates $\psi(t), \varphi(t)$ (or their estimated values $\hat{\psi}(t), \hat{\varphi}(t)$ from an observer/estimator) the controller outputs $i_\gamma(t), i_\delta(t)$ (i.e., the reference signals for the current controller) are determined by the relations

$$\begin{aligned}
\psi^*(t) &= \text{sat}\left(g^{-1}\left(L_r\,|T^*_{el}(t)|\right), \psi^*_{\min}, \psi^*_{\max}\right)\\
i_\psi(t) &= f^{-1}(\psi^*(t)) + \frac{k_\psi}{M}\left(\psi^*(t) - \hat{\psi}(t)\right)\\
i_\tau(t) &= \left(\frac{L_r}{M}\frac{T^*_{el}(t)}{\psi^*(t)^2} + \frac{k_p L_r}{R_r M}\left(T^*_{el}(t) - \hat{T}_{el}(t)\right)\right)\hat{\psi}(t)\\
i_\gamma(t) &= i_\psi(t)\cos\hat{\varphi}(t) - i_\tau(t)\sin\hat{\varphi}(t)\\
i_\delta(t) &= i_\psi(t)\sin\hat{\varphi}(t) + i_\tau(t)\cos\hat{\varphi}(t).
\end{aligned} \tag{41}$$

Remark 1. *If the nonlinear flux model (25) is used in combination with the modified equation for i_ψ from (41) the first equation of the closed loop model (17) changes to*

$$\dot{\psi} = -\tau_r^{-1}(Mf^{-1}(\psi) + k_\psi\psi) + \tau_r^{-1}(Mf^{-1}(\psi^*) + k_\psi\psi^*). \tag{42}$$

Since the inequality $Mf^{-1}(\psi) \geq \psi$ holds for all $\psi \geq 0$ it follows immediately that $\psi = 0$ is an asymptotically stable equilibrium of the unforced (i.e., for $\psi^*(t) = 0$) system (42). Additionally, using the Lyapunov functon $V = \frac{1}{2}\psi^2$ it can be shown that (42) has the so-called input to state stability property which means that $\psi(t)$ remains bounded whenever $\psi(0)$ and $\psi^*(t)$ are bounded [29]. Therefore, all results from the stability analysis of Section 3.2 remain valid.

5.1. Guidelines for Selection of Controller Parameters

The final control law (41) contains two parameters k_ψ and k_p which must have positive values in order to achieve stability of the closed loop system. Considering the dynamic capabilities of the controlled induction machine it would be desirable to select large values for k_ψ and k_p but of course this choice is limited by the constraint posed on the stator current vector. Therefore, some guidelines should be given next. Starting from the given maximum possible flux magnitude $\psi_{\max}$ we can determine the associated magnetization current amplitude $i_{\psi,m}$ via the measured magnetization curve, i.e., $i_{\psi,m} = f^{-1}(\psi_{\max})$. In order to achieve a desired dynamic flux control loop we may put the following constraint on the magnetization current

$$i_\psi \leq i_{\psi,\max} := 2i_{\psi,m.}$$

From (41) we have

$$i_\psi = f^{-1}(\psi^*) + \frac{k_\psi}{M}(\psi^* - \hat{\psi})$$

which immediately leads to the conservative constraint

$$f^{-1}(\psi_{\max}) + \frac{k_\psi}{M}\psi_{\max} \leq i_{\psi,\max}.$$

From this inequality we can derive a bound for the parameter k_ψ as

$$k_\psi \leq \frac{M}{\psi_{\max}}(i_{\psi,\max} - f^{-1}(\psi_{\max})) = \frac{M}{\psi_{\max}} i_{\psi,m}. \tag{43}$$

Given the maximum possible stator current amplitude $i_{\max}$ we can determine the maximum amplitude $i_{\tau,\max}$ of the torque producing current by

$$i_{\tau,\max} = \sqrt{i_{\max}^2 - i_{\psi,\max}^2}.$$

Now considering (15) it follows

$$|i_\tau| = \|\mathbf{i}_\tau\|_2 = \frac{\tau_r}{M}\left(s_3\tau_r^{-1} + k_p\tilde{T}_{el}\right)\psi$$

from which the inequality

$$(1 + k_p\tau_r\tilde{T}_{el}) \leq i_{\tau,\max}\frac{M}{\psi_{\max}}$$

can be derived. Under the assumption

$$\left|\tilde{T}_{el}\right| \leq 2T_{el,\max},$$

where $T_{el,\max}$ denotes the maximum possible torque, we get the desired bound

$$k_p \leq \frac{1}{2\tau_r T_{el,\max}}\left(i_{\tau,\max}\frac{M}{\psi_{\max}} - 1\right). \tag{44}$$

It should be emphasized that (43) and (44) are conservative bounds; therefore, the applied parameters may be increased to some extent.

5.2. Speed Control

The proposed torque control concept can be easily extended to speed control of an IM. In this case the mathematical model of the plant has to be augmented with the differential equation for the mechanical part of the system

$$J\dot{\omega}_m = -c\omega_m + T_{el} - T_l. \tag{45}$$

The inertia of the drive is denoted by J, c is a constant for viscous friction, and T_l is an unknown load torque. It is assumed that the mechanical speed ω_m can be measured. Now the proposed torque controller (41) can be simply extended by a speed controller whose output serves as reference torque input T_{el}^* for the torque controller. A standard PI-controller may be used for this purpose. The resulting structure of the controller including the flux and torque observer/estimator is shown in Figure 4. The reference signal for the mechanical speed is denoted by ω_m^*.

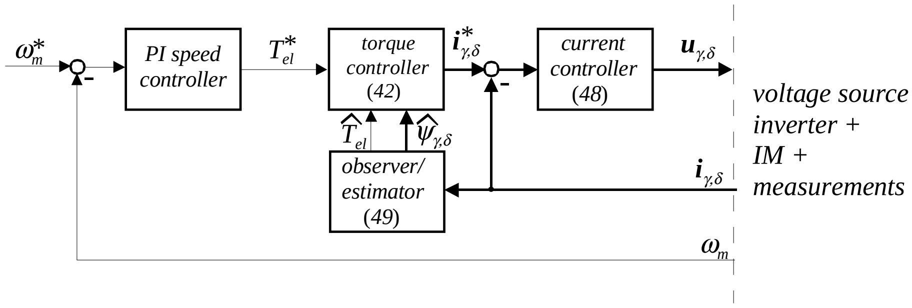

Figure 4. Controller structure for speed control.

For high performance servo applications it is preferable to choose ψ^* below the saturation point to ensure the required dynamic response. On the other hand, for slowly changing or constant speed references ω^* the flux command ψ^* could be optimized as proposed.

If we dispense with the maximum torque per ampere feature a simplified version of the speed controller can be derived from (41) in the following way: First (3) of the plant model is replaced by (45), next a suitable *constant* flux reference value ψ^* is chosen and finally the current component i_τ in (41) has to be modified such that it depends on the speed error. In this way the speed controller is given as:

$$\begin{aligned}
i_\psi(t) &= f^{-1}(\psi^*) + \frac{k_\psi}{M}\left(\psi^* - \hat{\psi}(t)\right)\\
i_\tau(t) &= \left(\frac{cL_r}{M}\frac{\omega_m^*(t)}{\psi^{*2}} + \frac{k_p L_r}{R_r M}\left(\omega_m^*(t) - \omega_m(t)\right)\right)\hat{\psi}(t)\\
i_\gamma(t) &= i_\psi(t)\cos\hat{\varphi}(t) - i_\tau(t)\sin\hat{\varphi}(t)\\
i_\delta(t) &= i_\psi(t)\sin\hat{\varphi}(t) + i_\tau(t)\cos\hat{\varphi}(t).
\end{aligned} \tag{46}$$

The closed loop system composed of (2), (45), and (46) is described by the relation (42) and

$$\begin{aligned}
\dot{\varphi} &= cR_r\frac{\omega_m^*}{\psi^{*2}} + k_p\left(\omega_m^* - \omega_m\right)\\
\dot{\omega}_m &= -\frac{1}{J}\left(c + \frac{k_p}{R_r}\psi^2\right)\omega_m\\
&\quad + \frac{1}{J}\left(c\frac{\psi^2}{\psi^{*2}} + \frac{k_p}{R_r}\psi^2\right)\omega_m^* - \frac{1}{J}T_l.
\end{aligned}$$

6. Control Implementation and Experimental Results

In the following, the practical implementation of the controller combined with the appropriate inner current control along with a rotor flux linkage estimator is considered. The current control that provides reference tracking, disturbance suppression, and voltage drop compensation of the Voltage Source Inverter (VSI) was realized in the rotor reference frame. The current error

$$\tilde{\mathbf{i}}_{\gamma,\delta} = \mathbf{i}^*_{\gamma,\delta} - \mathbf{i}_{\gamma,\delta}$$

was calculated from the reference currents obtained from the torque controller and the machine stator currents, that were directly measured. Based on an internal model principle a PI controller, that provides reference tracking and compensation of the back-EMF, was used in the following form:

$$\mathbf{u}_{\gamma,\delta} = k_{pi}\tilde{\mathbf{i}}_{\gamma,\delta} + k_{pi}k_{ii}\int_0^t \left(\frac{\mathbf{J}\omega_m}{k_{ii}} + \mathbf{I}\right)\tilde{\mathbf{i}}_{\gamma,\delta}d\tau \tag{47}$$

The constants $k_{pi}, k_{ii} > 0$ are free design parameters. In this application $k_{ii} = \tau_\sigma^{-1}$ was set. The implementation of the proposed control law clearly requires a rotor flux linkage estimator or observer. In experiments, a simplified magnetically nonlinear estimator was used based on the rotor model (25) in the following form

$$\begin{aligned}
i_\psi &= i_\gamma \cos\hat{\varphi} + i_\delta \sin\hat{\varphi} \\
i_\tau &= -i_\gamma \sin\hat{\varphi} + i_\delta \cos\hat{\varphi} \\
\dot{\hat{\psi}} &= \tau_r^{-1} M \left(-f^{-1}(\hat{\psi}) + i_\psi\right) \\
\dot{\hat{\varphi}} &= \tau_r^{-1} M \frac{i_\tau}{\hat{\psi}} \\
\dot{\hat{T}}_{el} &= -\tau_f^{-1}\hat{T}_{el} + \tau_f^{-1}\frac{M}{L_r}\hat{\psi} i_\tau.
\end{aligned} \tag{48}$$

The magnetization curve $\hat{\psi} = f(i_\psi)$ was implemented as lookup table.

The experimental setup consisted of the tested IM coupled with a separately controlled DC motor serving as variable load, a dSPACE PPC Controller board, a host PC with installed development environment, an incremental encoder with 5000 pulses per revolution, current sensors, voltage inverter, and a torque transducer. During tests, data acquisition, transformations, the flux, and torque estimator and the control algorithm were executed on the PowerPC with a sampling time of 250 µs, while a slave DSP was used for the vector modulation executed at 4 kHz. The program codes for the PowerPC and for the slave DSP were developed with the Real Time Interface and Simulink. Characteristic motor data and controller parameters for torque control are given in Table 1.

The first experiment presented in Figure 5 shows the machine response for a torque control with a piecewise constant torque reference and with adjusted rotor flux linkage magnitude as proposed in (31). The diagram (a) shows the estimated torque, the reference torque, and the filtered measured torque. For comparison on diagram (b), the same experiment is repeated using just the basic FOC (constant flux command, no compensation of magnetic nonlinearity, constant parameter flux estimator, current controllers in d-q reference frame, PI speed controller). Since no compensation of nonlinearity was used, some mismatch between observed, measured, and reference torque can be observed at higher torque values. Diagrams (c) and (d) show measured and reference currents while on the fifth diagram (e) the rotor flux linkage vector trajectory is shown. The last diagram (f) shows the reference and adjusted magnitude of the rotor flux linkage vector considering the nonlinear magnetizing characteristic.

Considering our previous proposition of the basic controller in (4), the advantages of the proposed extended control become evident if the reference changes sign with finite slope. This is illustrated for the reference profile that includes torque reversal in Figure 6. The proposed controller enables precise torque tracking also at zero crossings (a). On diagram (b) the comparison with FOC shows some deviation in the measured torque at higher reference values. Slightly better performance can be observed for the proposed control mostly due to the fact that just basic FOC was implemented. As in the previous experiment reference and measured currents (c,d), rotor flux linkage vector trajectory (e) and adjusted magnitude of the rotor flux linkage vector (f) are shown for the proposed control. Diagrams (g,h) show the stator current vector norms and corresponding integrals for a constant and optimized rotor flux. The current norm and the quantity E were obtained numerically from the measurements. For a constant rotor flux obtained with the proposed control and FOC the difference in E is a consequence of slightly bigger magnetizing current that was applied for a proposed control (curves 2 and 3). As expected, E is minimized for optimized rotor flux (curve 1). Similar performance could be achieved also with FOC for optimized rotor flux.

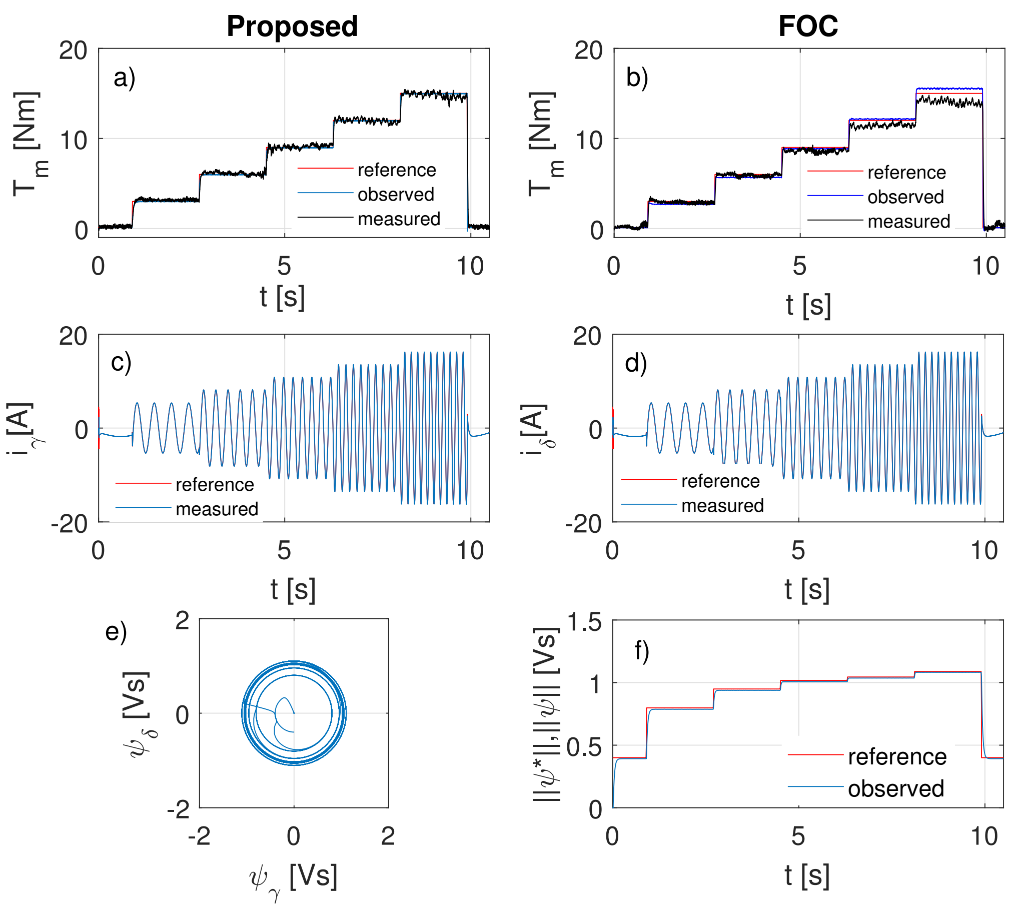

Figure 5. Torque control with adjusted rotor flux magnitude command and piecewise constant torque reference: torque response for proposed method (**a**), torque response for FOC (**b**), stator current components gamma and delta (**c**,**d**), rotor flux vector trajectory (**e**), rotor flux vector magnitude (**f**).

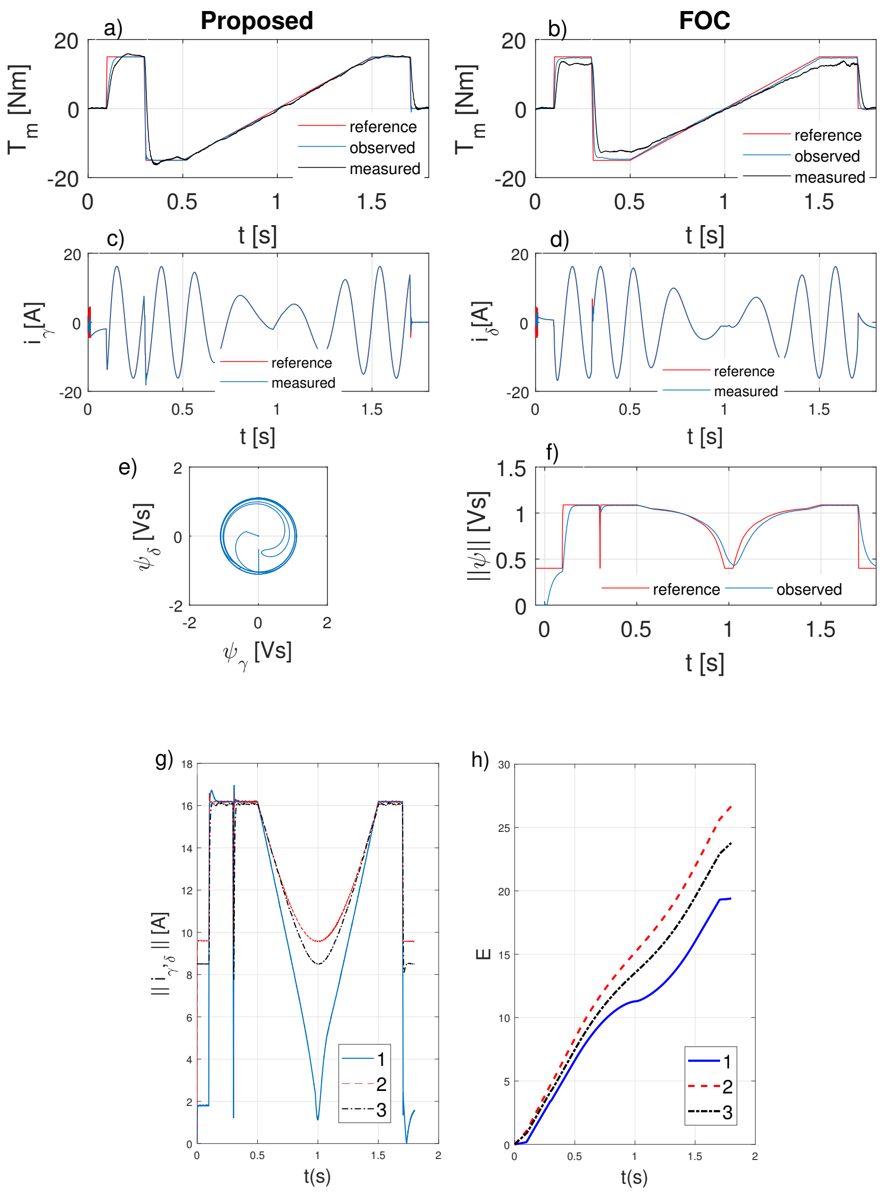

Figure 6. Torque control with optimized rotor flux magnitude command for the torque reversal including zero crossing with a finite slope (**a**–**f**) and comparison of stator current norm and corresponding integrals (**g**,**h**) for the proposed controller with optimized rotor flux (1) and with constant rotor flux (2) as well as for field oriented control (FOC) with constant rotor flux (3).

In Figure 7 the performance comparison for low speed reference is shown. No significant differences can be observed between proposed control and FOC. In the experiment shown in Figure 8 tracking performance for a harmonic speed reference with simultaneous constant load torque $T_l = -8$ Nm starting at $t = 1.9$ s is given. Actual and reference speed are shown in diagram (a), measured torque is given in diagram (b), while in diagrams (c) and (d) reference and measured currents i_γ and i_δ are shown. In Figure 9, the same variables as in the previous experiment are shown for a speed reversal command.

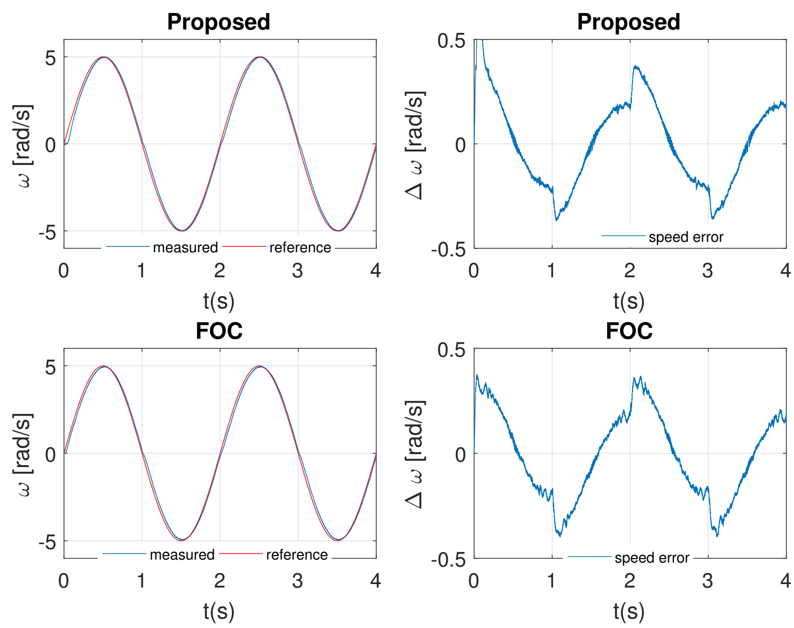

Figure 7. Performance comparison at low speed.

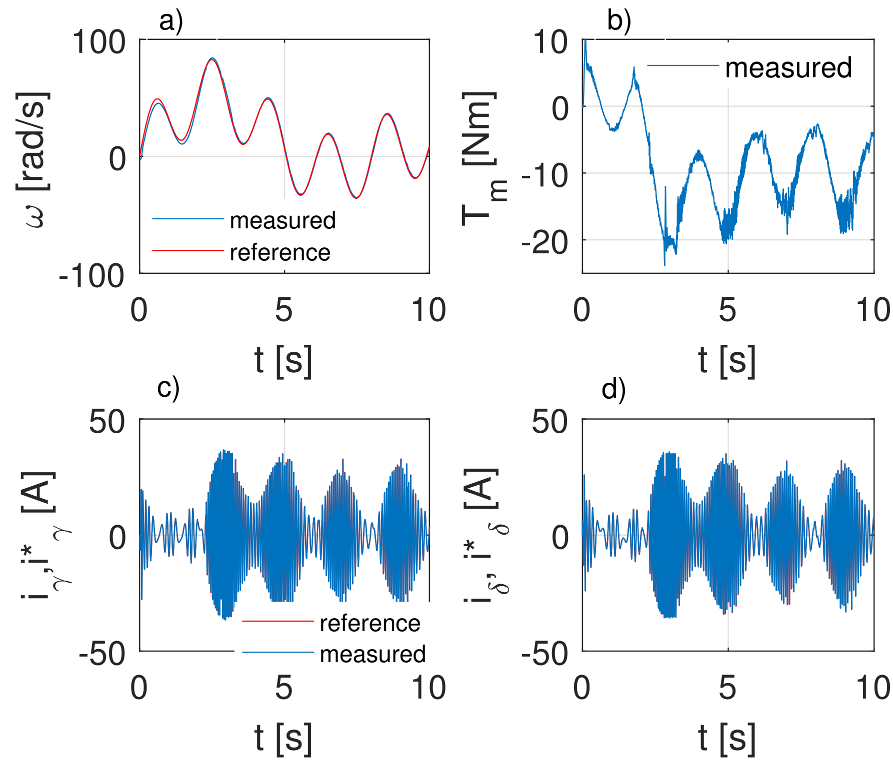

Figure 8. Speed response for harmonic speed reference and a constant load torque starting at $t = 1.9$ s: reference and measured speed (**a**), measured torque (**b**), reference and measured stator current vector components (**c**,**d**).

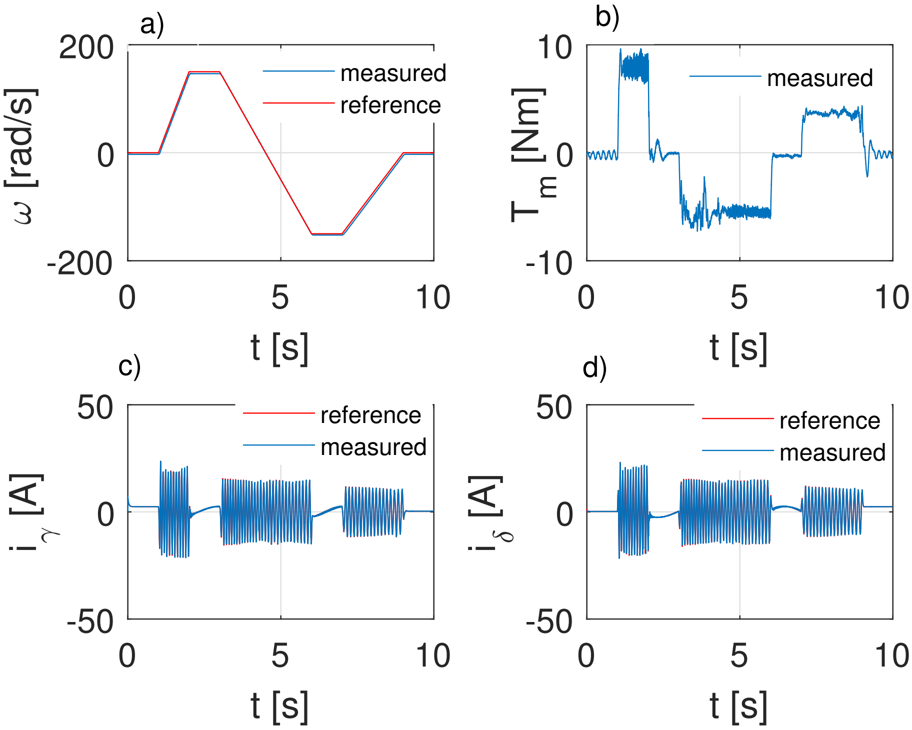

Figure 9. Control performance for the speed reversal command: speed response (**a**), measured torques (**b**), and reference and measured stator current vector components (**c**,**d**).

7. Conclusions

In this paper we proposed an extended controller for an induction machine based on the 3-D non-holonomic integrator that assures tracking of a general torque reference. This was achieved by extending a basic non-linear state controller with a separate control of the rotor flux linkage magnitude. The modified control results in a structure that is similar to FOC, although a completely different approach was used. It should be pointed out that brief additional results obtained with classical FOC are given exclusively to show that similar overall performance could be obtained with the proposed approach and are not meant for detail performance evaluation or comparison. The additional control loop in proposed control scheme provides extra flexibility to meet performance requirements posed on the drive. As occasion demands the rotor flux linkage magnitude can be optimized to assure energy efficiency or can be kept constant to provide high dynamic tracking performance in servo applications. It follows from our experience that both requirements are hard to satisfy simultaneously without prior information about the class of reference signals. Simultaneous online optimization of the flux magnitude for completely arbitrary torque reference is computationally still too demanding for existing hardware. With the proposed controller, singularity problems of the original controller (4) are completely removed. Since the nonlinear state controller requires a rotor flux linkage estimate, further improvement could be achieved by implementing well known estimation techniques in the proposed control.

Author Contributions: Conceptualization, B.G. and A.H.; writing—original draft preparation, B.G. and A.H.; experimental validation, G.Š.; writing—review and editing, G.Š. All authors have read and agreed to the published version of the manuscript.

Funding: This work was supported in part by the Slovenian Research Agency, project no. P2-0115 and J2-1742.

Conflicts of Interest: The authors declare no conflict of interest.

References

1. Marino, R.; Peresada, S.; Tomei, P. Global Adaptive Output Feedback Control of Induction Motors with Uncertain Rotor Resistance. *IEEE Trans. Autom. Control* **1999**, *44*, 964–980. [CrossRef]
2. Bodson, M.; Chiasson, J. Differential-Geometric Methods for Control of Electric Motors. *Int. J. Robust Nonlinear Control* **1998**, *8*, 927–952. [CrossRef]
3. Oteafy, A.; Chiasson, J. Lyapunov stability of an open-loop induction machine. In Proceedings of the American Control Conference, St. Louis, MO, USA, 10–12 June 2009; pp. 3452–3457.
4. Ortega, R.; Loria, A.; Nicklasson, P.J.; Siera-Ramirez, H. Current fed induction motors. In *Passivity-Based Control of Euler-Lagrange Systems*; Springer: Berlin, Germany, 1998; pp. 381–439.
5. Peresada, S.; Tilli, A.; Tonielli, A.Current regulation strategies for vector-controlled induction motor drives. *IEEE Trans. Power Electron.* **2003**, *18*, 151–163. [CrossRef]
6. Holmes, D.G.; McGrath, B.P.; Parker, S. Current regulation strategies for vector-controlled induction motor drives. *IEEE Trans. Ind. Electron.* **2012**, *59*, 3680–3689. [CrossRef]
7. Hajian, M.; Soltani, J.; Markadeh, G.A.; Hosseinnia, S. Adaptive nonlinear direct torque control of sensorless IM drives with efficiency optimization. *IEEE Trans. Ind. Electron.* **2010**, *57*, 975–985. [CrossRef]
8. Casadei, D.; Member, S.; Serra, G.; Stefani, A.; Tani, A.L. Zarri, L. DTC drives for wide speed range applications using a robust flux-weakening algorithm. *IEEE Trans. Ind. Electron.* **2007**, *54*, 2451–2461. [CrossRef]
9. Alexandridis, A.T.; Konstantopoulos, G.C.; Zhong, Q.-C. Advanced integrated modeling and analysis for adjustable speed drives of induction motors operating with minimum losses. *IEEE Trans. Energy Convers.* to be published. [CrossRef]
10. Stojić, D.; Milinković, M.; Veinović, S.; Klasnić, I. Improved stator flux estimator for speed sensorless induction motor drives. *Ieee Trans. Ind. Electron.* **2015**, *30*, 2363–2371. [CrossRef]
11. Canudas de Wit, C.; Ramirez, J. Optimal Torque Control for Current-Fed Induction Motors. *IEEE Trans. Autom. Control* **1999**, *44*, 1084–1089. [CrossRef]
12. Fernández-Bernal, F.; García-Cerrada, A.; Faure, R. Model-Based Loss Minimization for DC and AC Vector-Controlled Motors Including Core Saturation. *IEEE Trans. Ind. Appl.* **2000**, *36*, 755–763. [CrossRef]
13. Stumper, J.F.; Dötlinger, A.; Kennel, R. Loss Minimization of Induction Machines in Dynamic Operation. *IEEE Trans. Energy Convers.* **2013**, *28*, 726–735. [CrossRef]
14. Borisevich, A.; Schullerus, G. Energy Efficient Control of an Induction Machine Under Torque Step Changes. *IEEE Trans. Energy Convers.* **2016**, *31*, 1295–1303. [CrossRef]
15. Schnurr, C.; Hohmann, S.; Kolb, J. Non-linear MPC for winding loss optimised torque control of anisotropic PMSM. *J. Eng.* **2018**, *17*, 4252–4256. [CrossRef]
16. Brockett, R. Characteristic phenomena and model problems in nonlinear control. *IEEE Trans. Autom. Control* **1998**, *48*, 391–396. [CrossRef]
17. Hespanha, J.P.; Morse, A.S. Stabilization of nonholonomic integrators via logic-based switching. *Automatica* **1999**, *35*, 385–393. [CrossRef]
18. Morgansen, K.A. Controllability and trajectory tracking for classes of cascade-form second order nonholonomic systems. In Proceedings of the 40th IEEE Conference on Decision and Control, Orlando, FL, USA, 4–7 December 2001; pp. 3031–3036.
19. Bloch, A.; Drakunov, S. Stabilization and tracking control in the nonholonomic integrator via sliding modes. *Syst. Control Lett.* **1996**, *29*, 91–99. [CrossRef]
20. Xua, W.L.; Huob, W. Variable structure exponential stabilization of chained systems based on the extended nonholonomic integrator. *Syst. Control Lett.* **2000**, *41*, 225–235. [CrossRef]
21. Grčar, B.; Cafuta, P.; Štumberger, G.; Stankovič, A.; Hofer, A. Non-holonomy in Induction Torque Control. *IEEE Trans. Control Syst. Technol.* **2011**, *19*, 367–375. [CrossRef]
22. Grčar, B.; Hofer, A.; Cafuta, P.; Štumberger, G. A contribution to the control of the non-holonomic integrator including drift. *Automatica* **2012**, *48*, 2888–2893. [CrossRef]
23. Hofer, A.; Grčar, B.; Štumberger, G.; Horn, M.; Reichhartinger, M. Führungsregelung für den nichtholonomen Integrator mit Drift. *Automatisierungstechnik* **2015**, *63*, 700–712.
24. Chen, C.T. *Linear System Theory and Design*; Oxford University Press: Oxford, UK, 1984.

25. Heinemann, G.; Leonhard, W. Self-tuning field-oriented control of an induction motor drive. In Proceedings of the International Power Electronics Conference, Tokyo, Japan, 2–6 April 1990.
26. Novotnak, R.T.; Chiasson, J.; Bodson, M. High-Performance Motion Control of an Induction Motor with Magnetic Saturation. *IEEE Trans. Control Syst. Technol.* **1999**, *7*, 315–327. [CrossRef]
27. Atans, M.; Falb, P.L. *Optimal Control*; McGraw-Hill Book Company: New York, NY, USA, 1966.
28. Shampine, L.F.; Kierzenka, J.; Reichelr, M.W. *Solving Boundary Value Problems for Ordinary Differential Equations in MATLAB with bvp4c*; The MathWorks Inc.: Natick, MA, USA, 2000.
29. Sontag, E.D. Smooth stabilization implies coprime factorization. *IEEE Trans. Autom. Control* **1989**, *34*, 435–443. [CrossRef]